Received: 27 May 2020 | Revised: 9 October 2020 | Accepted: 12 October 2020

DOI: 10.1111/pce.13915

ORIGINAL ARTICLE

Plant, Cell & Environment WILEY

Seasonal and diurnal trends in progressive isotope enrichment along needles in two pine species

Steven A. Kannenberg[1] | Richard P. Fiorella[2] | William R. L. Anderegg[1] | Russell K. Monson[3] | James R. Ehleringer[1]

[1]School of Biological Sciences, University of Utah, Salt Lake City, Utah

[2]Department of Geology and Geophysics, University of Utah, Salt Lake City, Utah

[3]Department of Ecology and Evolutionary Biology, University of Colorado Boulder, Boulder, Colorado

Correspondence
Steven A. Kannenberg, School of Biological Sciences, University of Utah, Salt Lake City, UT 84112, USA.
Email: s.kannenberg@utah.edu

Funding information
David and Lucille Packard Foundation; National Science Foundation, Grant/Award Numbers: 1714972, 1753845, 1754430, 1802880; USDA, Grant/Award Number: 2018-67019-27850

Abstract

The Craig–Gordon type (C–G) leaf water isotope enrichment models assume a homogeneous distribution of enriched water across the leaf surface, despite observations that $\Delta^{18}O$ can become increasingly enriched from leaf base to tip. Datasets of this 'progressive isotope enrichment' are limited, precluding a comprehensive understanding of (a) the magnitude and variability of progressive isotope enrichment, and (b) how progressive enrichment impacts the accuracy of C–G leaf water model predictions. Here, we present observations of progressive enrichment in two conifer species that capture seasonal and diurnal variability in environmental conditions. We further examine which leaf water isotope models best capture the influence of progressive enrichment on bulk needle water $\Delta^{18}O$. Observed progressive enrichment was large and equal in magnitude across both species. The magnitude of this effect fluctuated seasonally in concert with vapour pressure deficit, but was static in the face of diurnal cycles in meteorological conditions. Despite large progressive enrichment, three variants of the C–G model reasonably successfully predicted bulk needle $\Delta^{18}O$. Our results thus suggest that the presence of progressive enrichment does not impact the predictive success of C–G models, and instead yields new insight regarding the physiological and anatomical mechanisms that cause progressive isotope enrichment.

KEYWORDS

Craig–Gordon, desert river, Péclet, *Pinus contorta*, *Pinus ponderosa*, stable isotopes

1 | INTRODUCTION

Variation in the isotopic enrichment of evaporating leaf water is a key indicator of leaf-level plant physiology and has numerous applications, such as quantifying historical responses to climate variability (Kahmen, Schefuß, & Sachse, 2013; Roden, Lin, & Ehleringer, 2000), assessing the geographic origin of plant material (Dawson, Mambelli, Plamboeck, Templer, & Tu, 2002), and interpreting the isotopic composition of atmospheric CO_2 and O_2 (Dole, Lane, Rudd, & Zaukelies, 1954; Welp et al., 2011). As such, a rich history of research has used evaporative enrichment models (e.g. Dongmann, Nurnberg, Forstel, & Wagener, 1974; Farquhar & Cernusak, 2005; Farquhar & Gan, 2003; Flanagan, Comstock, & Ehieringer, 1991; Leaney, Osmond, Allison, & Ziegler, 1985; Ogée, Cuntz, Peylin, & Bariac, 2007; Song, Loucos, Simonin, Farquhar, & Barbour, 2015) to predict temporal variation in leaf water isotopic enrichment in response to changing environmental conditions. These models all are based on the classic Craig–Gordon (C–G) model for evaporation from open water surfaces, modified for leaves (Craig & Gordon, 1965).

Early evaporative enrichment models were developed to predict bulk leaf water enrichment (i.e. the aggregated enrichment observed when considering all water present in a leaf). Observations have

revealed, however, that leaf water isotope ratios are often spatially heterogenous. Most commonly, it has been shown that the $\delta^{18}O$ of leaf water is progressively more enriched from base to tip and from midrib out to leaf edge (Gan, Wong, Ong, & Farquhar, 2003; Gan, Wong, Yong, & Farquhar, 2002; Helliker & Ehleringer, 2000; Šantrůček, Květoň, Šetlík, & Bulíčková, 2007; Wang & Yakir, 1995). The magnitude of this 'progressive enrichment' is quite striking in some studies, as the spatial variation of $\delta^{18}O$ enrichment in the water of a single leaf at one point in time often exceeds the amount of temporal variation observed across all environmental conditions (Helliker & Ehleringer, 2000; Šantrůček et al., 2007; Shu, Feng, Posmentier, Faiia, et al., 2008).

Several models have been developed to capture the observed spatial variability in leaf water enrichment along the length of the leaf (Cuntz, Ogée, Farquhar, Peylin, & Cernusak, 2007; Farquhar & Gan, 2003; Helliker & Ehleringer, 2000; Ogée et al., 2007; Shu, Feng, Posmentier, Sonder, et al., 2008). These models all rely on a key concept to generate progressive enrichment: that the heavy isotopologue of water can diffuse back into the leaf from the evaporation site (i.e. the mesophyll surfaces near the stomatal pore) into the unenriched source water, and this newly enriched source water can then be transported to more distal evaporation sites where the cycle of enrichment and back-diffusion can begin anew. Beyond this fundamental mechanism, however, each of the models differs in their predictions regarding what causes variability in the magnitude of the progressive isotope enrichment effect. For this process to occur, it has been suggested that radial advection of water towards the evaporation site (the normal flow in a transpiring leaf) needs to be slow enough to not overwhelm back-diffusion of the heavy isotopologue, leading to predictions that this phenomenon should only be present in species with small interveinal distances (Helliker & Ehleringer, 2000) and/or large mesophyll tortuosity (Farquhar & Gan, 2003; Ogée et al., 2007). Other factors have been suggested to increase the strength of longitudinal progressive enrichment, such as a longer leaf length (Helliker & Ehleringer, 2000; Roden, Kahmen, Buchmann, & Siegwolf, 2015), low humidity and high transpiration rates (Farquhar & Gan, 2003; Gan et al., 2002, 2003; Šantrůček et al., 2007). A detailed evaluation of these predictions has not been possible because of the dearth of observational datasets. As a result, we currently lack a comprehensive understanding of the ubiquity, variability and mechanistic basis of progressive enrichment of leaf water isotopes.

While progressive enrichment leads to a heterogeneous distribution of isotope ratios, it theoretically should not directly influence evaporative fractionation of bulk leaf water. However, bulk leaf water modelling in conifers is subject to numerous uncertainties (Belmecheri, Wright, Szejner, Morino, & Monson, 2018; Roden et al., 2015) that are potentially exacerbated by variability in progressive enrichment. Unfortunately, a lack of studies that pair C–G leaf water modelling with a quantification of progressive enrichment has limited comprehensive tests of the ability of C–G models to accurately predict bulk leaf water fractionation in leaves with significant enrichment gradients. Moreover, many of the anatomical, physiological and meteorological drivers of variation in progressive enrichment are not fully understood, hindering our ability to model progressive isotope enrichment across a diverse assemblage of species and environmental conditions. Knowledge of the conditions that cause variation in progressive enrichment may be crucial for understanding and predicting the frequent decoupling between bulk leaf water enrichment and isotopic ratios of downstream metabolic products (Barnard et al., 2007; Gessler et al., 2013; Lehmann, Gamarra, Kahmen, Siegwolf, & Saurer, 2017).

In order to understand the magnitude and variability of progressive isotope enrichment, and to understand how this process impacts our ability to accurately model bulk leaf water isotopic enrichment, we collected an extensive dataset of the spatial variability in $\delta^{18}O$ along the length of conifer needles. Over a 2-year period, we measured leaf water $\delta^{18}O$ along discrete needle segments in two different species (*Pinus ponderosa* and *Pinus contorta*) on both a diurnal and seasonal basis, encompassing a wide range of meteorological and phenological conditions. We further sought to understand the degree to which various C–G based models successfully capture trends in bulk leaf water isotope ratios irrespective of the progressive enrichment effect. Specifically, we ask:

1. Is progressive isotope enrichment present across two conifer species and how much does this effect vary seasonally and diurnally?
2. What environmental drivers determine variation in the degree to which progressive enrichment occurs? Do these drivers suggest potential mechanisms?
3. Which C–G model is best able to predict bulk leaf isotope ratios in the presence of seasonal and diurnal variability in progressive enrichment?

2 | MATERIALS AND METHODS

2.1 | Study site and general sampling approach

Throughout 2018 and 2019, we sampled mature populations of *P. contorta* and *P. ponderosa* in Big Cottonwood Canyon, Salt Lake City, UT (40°38′37.1″N, 111°38′17.4″W). All sampled trees were no farther than 100 m from each other and located on the same slope and aspect. The *P. ponderosa* trees chosen for sampling were ~35 cm diameter at breast height and 15 m tall, while the *P. contorta* trees were ~20 cm in diameter and 5 m tall. Three different types of samples were collected: (a) stem xylem samples to quantify shifts in source water $\delta^{18}O$, (b) whole needle samples to test bulk leaf water model predictions, and (c) discrete needle segments to quantify the magnitude of the progressive enrichment effect. Stem samples (the first ~2 cm of sapwood) were extracted using an increment borer, whole needle samples (5–10 needles per sampling time) were harvested by hand, and needle segments were obtained by immediately sectioning 5–10 additional whole needle samples into thirds. All sampled needles were exposed to full sunlight, and were 1–2 years old to standardize the length of needle segments and to avoid any effects associated with new needle expansion. Following sampling, all wood and needle samples were placed in a glass vial within

30 seconds, capped, sealed with parafilm, and stored on ice until transported to a −20°C freezer within 18 hr for longer-term storage before analyses could be conducted.

2.2 | Annual sampling protocols

In 2018, stem cores were sampled at 11 time points throughout the summer and fall in *P. ponderosa* (Figure S1). Additionally, on 5 September we sampled needle segments at four time points (0500, 0900, 1300 and 1600 hr) in three different trees in order to quantify diurnal variation in the progressive isotope enrichment effect in both *P. contorta* and *P. ponderosa*. On this date, stem core samples were also taken for both species. In 2019, five *P. ponderosa* trees were sampled throughout the summer and fall. Stem samples were obtained at 1300 hr on seven different days between May and October (Figure S1), while whole needle samples were obtained at three time points diurnally (0900, 1300 and 1600 hr) on these dates (Figure 1).

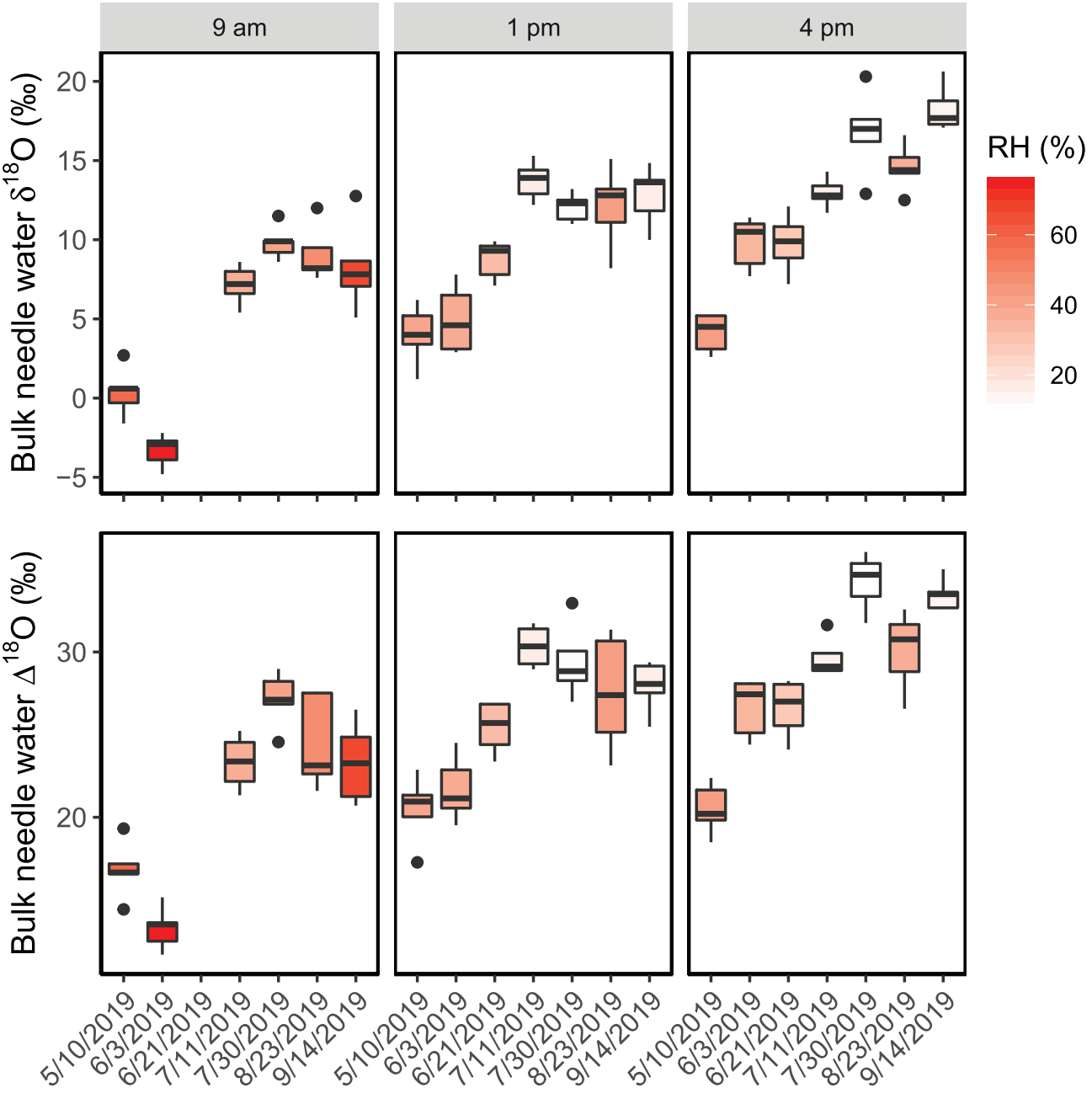

FIGURE 1 Bulk needle water $\delta^{18}O$ and bulk needle water $\Delta^{18}O$ in *P. ponderosa* across all sampling times (0900, 1300 and 1600 hr) and dates. $n = 5$ for all sampling times and dates. Colour indicates the RH at the hour of sampling on each day. Horizontal lines within each box represent the median, boxes represent the limits of the lower and upper quartiles, vertical lines represent upper and lower ranges and dots represent outliers [Colour figure can be viewed at wileyonlinelibrary.com]

On these days, we also measured water potential on individual needle fascicles between 1200 and 1300 hr using a Scholander-type pressure chamber (PMS Instruments, Corvallis, OR). Additionally, on 21 June we quantified diurnal variation in the progressive isotope enrichment effect (as described above) in all five trees. Finally, we quantified seasonal variation in the progressive enrichment effect by sampling needle segments at 1300 hr on three additional dates throughout the year.

2.3 | Weather data

Weather data (air temperature and relative humidity) were obtained from the Utah Department of Transportation Cardiff—Big Cottonwood Canyon (site code: UTCDF) weather station (1.5 km northwest of our site at a similar elevation) as part of the University of Utah MesoWest network (mesowest.utah.edu, Horel et al., 2002). When necessary, data gaps from this station were filled using linear regression with data from a nearby MesoWest site (Utah Department of Transportation White Pine—Little Cottonwood Canyon weather station, site code: UTWLC, ~8 km away). The UTWLC site is in a canyon adjacent to the study site, and at similar elevation and aspect.

2.4 | Water extraction and $\delta^{18}O$ analysis

Within 3 months of collection, water was extracted from stem and needle samples using cryogenic vacuum distillation with a boiling water bath and a vacuum pressure of less than 100 mTorr (Ehleringer, Roden, & Dawson, 2000). Extractions were performed for at least 60 min for needle samples and 90 min for stem samples to ensure full extraction (West, Patrickson, & Ehleringer, 2006). All water samples were analysed for $\delta^{18}O$ through the Stable Isotope Research Facility for Environmental Research at the University of Utah. Oxygen isotope ratios of extracted water samples were determined with a high temperature elemental analyser coupled to a ConFlo III referencing interface and a DeltaPlusXL isotope ratio mass spectrometer (TC/EA–IRMS, all supplied by Finnigan MAT, Bremen, Germany), using a glassy carbon pyrolysis method as previously described (Gehre, Geilmann, Richter, Werner, & Brand, 2004). Aliquots of 0.5–1 μL of water samples were injected with an autosampler (GC-PAL, Zwingen, Switzerland) equipped with a gas-tight syringe. Due to instrument malfunctions, some water samples had to be analysed using a CO_2 equilibration technique, whereby 0.2 mL of water sample was injected into 11 mL exetainers, which were then flushed with a mixture of 0.5% CO_2 and 95.5% He using a double capillary needle. The samples were then held in a temperature-controlled autosampler to equilibrate for 24 hr, and analysed using a Gas-Bench II connected to a Delta Plus XL (Finnigan MAT, Bremen, Germany). No differences in the statistical properties of our isotope ratio data were detected between samples analysed with the CO_2 equilibration versus pyrolysis techniques. Isotope ratios were measured on the resulting gas and referenced to the international VSMOW standard (IAEA, Vienna, Austria). Measurement precision of quality control standards were <0.1‰ SD, and sample data were normalized as per Nelson (2000) in order to account for systematic error.

Isotope ratios are expressed as part-per-thousand deviations from the VSMOW standard using lower-case delta notation (δ, in per mil):

$$\delta = \left(\frac{R_{\text{sample}}}{R_{\text{standard}}} - 1\right), \tag{1}$$

where R_{sample} and R_{standard} are the ratios of ^{18}O to ^{16}O in the sample and the VSMOW standard (2000.5×10^{-6}), respectively. Alternatively, isotope ratios are considered as enrichments above xylem water using capital delta notation (Δ) to remove apparent variations associated with changes in source water isotope ratios:

$$\Delta^{18}O = \frac{\delta^{18}O_{\text{leaf}} - \delta^{18}O_{\text{xylem}}}{1 + \delta^{18}O_{\text{xylem}}}. \tag{2}$$

2.5 | Leaf water isotope modelling: Bulk leaf water

The most widely used leaf water models are based on a modified form of the C–G model for evaporation, originally developed to explain isotope ratios of water vapour (R_E) evaporating from the ocean surface (Craig & Gordon, 1965):

$$R_E = \frac{\alpha_K\left(\frac{R_L}{\alpha_{eq}} - hR_V\right)}{1-h}, \tag{3}$$

where R_L, and R_V are the isotope ratios of water in the evaporating liquid pool (in this case, the leaf water) and atmospheric water vapour, α_K and α_{eq} are the kinetic (Merlivat, 1978) and temperature-dependent liquid vapour equilibrium fractionations (Horita & Wesolowski, 1994), and h is the ratio of atmospheric vapour pressure to the saturation vapour pressure at the leaf temperature. If leaf and air temperature are equal, h is equivalent to relative humidity. If we assume the leaf is at isotopic steady-state, where the isotope ratio of the evaporative flux (R_E) is equal to the isotope ratio of xylem water entering the leaf (R_X), this equation can be rearranged to approximate the isotope ratio of leaf water in Δ notation, where Δ_C is the enrichment of evaporative site water above source water, ε^+ and ε_k are the equilibrium and kinetic fractionations (Merlivat, 1978), respectively, and w_a/w_i is relative humidity under the assumption that leaf and air temperature are equivalent (Dongmann et al., 1974):

$$\Delta_C \approx \varepsilon^+ + \varepsilon_k + (\Delta_v - \varepsilon_k)\frac{w_a}{w_i}. \tag{4}$$

The C–G model captures first-order controls on leaf isotope ratios well (e.g. (Roden & Ehleringer, 1999), but several studies have demonstrated that the C–G model tends to overestimate observed bulk leaf water isotope ratios (Cernusak et al., 2016). This observation has led

to two different corrections to explain this difference. Firstly, it has been suggested that two discrete water 'pools' may exist in leaves (Yakir, DeNiro, & Gat, 1990): water that has been evaporatively enriched and thus can be modelled by the C–G equations, and an unenriched water pool present in veins that transport water to the sites of evaporation. The bulk leaf water isotope ratio (Δ_L) can then be represented by a mixing model:

$$\Delta_L = \Delta_C(1-f_u), \tag{5}$$

where Δ_C is the C–G derived isotope ratio of water at the sites of evaporation and f_u is the fraction of unenriched water in the leaf.

Secondly, it has been suggested that this pattern may be evidence of a Péclet effect, where the isotope ratio of water in leaf lamina reflects the balance between advection of water into the lamina and the diffusion of heavy isotopologues away from the sites of enrichment. To account for this phenomenon, the C–G prediction is modified as:

$$\Delta_L = \frac{\Delta_C(1-e^{-\wp})}{\wp}, \tag{6}$$

where $\wp$ is the Péclet number reflecting the ratio of advective-to-diffusive transport in the leaf (Farquhar & Lloyd, 1993):

$$\wp = \frac{EL}{CD}, \tag{7}$$

where E is the transpiration rate, L is the effective path length (m), C is the molar density of water (55.5×10^3 mol/m^3), and D is the temperature-dependent (e.g. Cuntz et al., 2007) diffusivity of water (m^2/s), where T is temperature (°C):

$$D = 97.5 \times 10^{-9} \exp\left(-\frac{577}{T+128}\right). \tag{8}$$

For transpiration rate, we used a mean value across all conditions (1.3×10^{-3} mol m^2 s^{-1}) from a study on mature *P. ponderosa*, also located in the southwestern United States (Kolb, Holmberg, Wagner, & Stone, 1998).

2.6 | Leaf water isotope modelling: Model of progressive isotope enrichment

The maximum bulk leaf water $\delta^{18}O$ ratio predicted by the models described above would be provided by the unmodified C–G equation. While the C–G model is known to generally overestimate bulk leaf water $\delta^{18}O$ values, some studies have reported water isotope ratios in portions of leaves above C–G predictions (e.g. Cernusak et al., 2016). To account for this, Farquhar and Gan (2003) described enrichment along the length of a leaf in a continuous fashion as a 'desert river', where water evaporates continuously along a path until it is completely evaporated. In this formulation (Equation (5) from Farquhar & Gan, 2003), the isotope ratio at any point along the leaf can be expressed as:

$$\Delta_L(l) = \frac{\Delta_C}{h'}\left[1-\left(1-\frac{l}{l_m}\right)^{\frac{h'}{1-h'}}\right], \tag{9}$$

where Δ_C is the predicted bulk leaf water isotope ratio from the standard C–G equation, l is the position along the leaf, l_m is the length of the leaf, and $h' = 1 - \alpha_{eq}\alpha_k(1-h)$. The maximum enrichment observed in the leaf, located at l_m, has an isotope ratio of Δ_C/h'. When integrated over the whole leaf, this model yields an average value equivalent to C–G prediction (Farquhar & Gan, 2003).

2.7 | Estimation of the isotope ratio of the atmospheric water vapour, δ_V

Accurate prediction of leaf water isotope ratios in all of these formulations requires knowledge of the atmospheric water vapour isotope ratio, δ_V. δ_V is often assumed to be in equilibrium with local precipitation or plant xylem water, though a recent evaluation of this relationship with simulated water isotope ratios in general circulation models suggested that water vapour isotope ratios are often higher than would be expected from the equilibrium assumption due to large-scale atmospheric mixing (Fiorella, West, & Bowen, 2019). Therefore, atmospheric water vapour isotope ratios should be measured rather than assumed, where possible. Water vapour isotope ratios have been measured on the University of Utah campus, ~22 km northwest of the study site, using a Picarro L2130-i since December 2013 (Fiorella, Bares, Lin, Ehleringer, & Bowen, 2018). Unfortunately, this analyser malfunctioned during most of the 2019 summer, limiting data availability. As a result, we have made three different assumptions regarding δ_V in our calculations: (a) that δ_V was in equilibrium with δ_x, (b) considering δ_V as monthly values from previous years (2014–2017), and (c) estimating $\delta_V$via relationships between δ_V, vapour pressure, and relative humidity from 2014 to 2017 ($\delta^{18}O_V = -29.44 - 62.8 \times 10^{-2} RH + 5.283 ln(vp)$, $r^2 = 0.50$, $p < 2 \times 10^{-16}$, RH in percent, vp in hPa). We used both RH and vp in this model because they capture slightly different biophysical processes, and were decoupled in the data on which this equation was developed [$R = 0.02$ for a linear model between ln(vp) and RH]. Estimated values using these three approaches are shown in Table S1. In general, all three assumptions resulted in C–G model predictions that were similar (Figure S2). While the assumption that δ_V was in equilibrium with δ_x provided the best fit to our data, this is likely because of compensating errors (i.e. the C–G model tends to overpredict leaf $\delta^{18}O$ while the equilibrium assumption tends to underpredict $\delta^{18}O_V$). Considering that the model predictions using the other two assumptions had identical RMSE and R^2, for all analysis we elected to use the regression-predicted values of $\delta^{18}O_V$.

2.8 | Statistical analyses

Relationships between enrichment patterns and meteorological conditions were assessed via ordinary least squares linear regression, while differences in the progressive isotopic enrichment effect and enrichment patterns across needle segments were discerned using pairwise comparisons via Tukey's HSD. Normality and homoscedasticity of residuals was confirmed using quantile–quantile plots. We parameterized the isotope models (specifically f_u for the 2-pool C–G model and L for the Péclet modification) in order to minimize RMSE across all data points. All modelling and statistical analysis was done in R 3.6 (R Core Team, 2019).

3 | RESULTS

3.1 | Stem and bulk leaf water enrichment

The seasonal patterns of *P. ponderosa* stem water $\delta^{18}O$ differed across both sampling years. In 2018, stem $\delta^{18}O$ gradually decreased over the course of the growing season while in 2019 $\delta^{18}O$ was relatively constant until a slight increase occurred in late August and early September (Figure S1). In 2019, $\delta^{18}O$ and $\Delta^{18}O$ in bulk needle water sampled at 1300 hr generally increased throughout the season (Figure 1), primarily responding to the seasonal trend of decreases in midday relative humidity (RH, $p < .0001$, $R^2 = 0.40$). Decreases in RH diurnally also increased bulk needle water $\Delta^{18}O$ within individual days, as we observed strong negative relationships between RH and $\Delta^{18}O$ within every day where we sampled needles in the morning, afternoon, and evening (all $p < .01$, R^2 range: 0.43–0.85).

3.2 | Magnitude and variation of progressive isotope enrichment

The magnitude of progressive isotope enrichment (i.e. the difference between needle base $\delta^{18}O$ and needle tip $\delta^{18}O$) in *P. ponderosa* needles was large and seasonally variable, ranging from a 22.3‰ in early 2019 to 44.3‰ by late 2019 (Figure 2). Across all sampling points, the magnitude of progressive enrichment was larger than the variation in bulk needle water $\delta^{18}O$ associated with diurnal and seasonal fluctuations (Figure 1). Seasonal variation in the magnitude of midday progressive isotope enrichment was related primarily to RH ($p < .0001$, $R^2 = 0.89$) and leaf water potential ($p < .0001$, $R^2 = 0.79$) at the time of sampling. In general, needle water $\Delta^{18}O$ in the middle segment and top segment increased over the course of the year, while needle water $\Delta^{18}O$ in the bottom segment remained comparatively static (Figure 3). Bulk needle water $\Delta^{18}O$ most closely matched $\Delta^{18}O$ in the middle needle segment throughout 2019 (Figure 3).

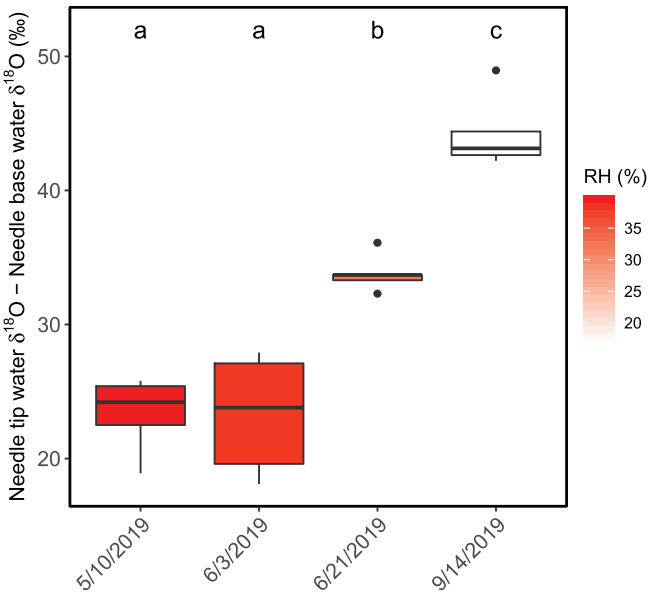

FIGURE 2 The magnitude of the progressive isotope enrichment across the needle (i.e. the difference between needle tip and base $\delta^{18}O$ in ‰) for *P. ponderosa*. $n = 5$ for all sampling dates at 1300 hr. Letter notation indicates significant pairwise differences between the magnitude of progressive enrichment across all sampling dates (adjusted $\alpha = .05$). Colour indicates the RH at the hour of sampling on each day. Horizontal lines within each box represent the median, boxes represent the limits of the lower and upper quartiles, vertical lines represent upper and lower ranges and dots represent outliers [Colour figure can be viewed at wileyonlinelibrary.com]

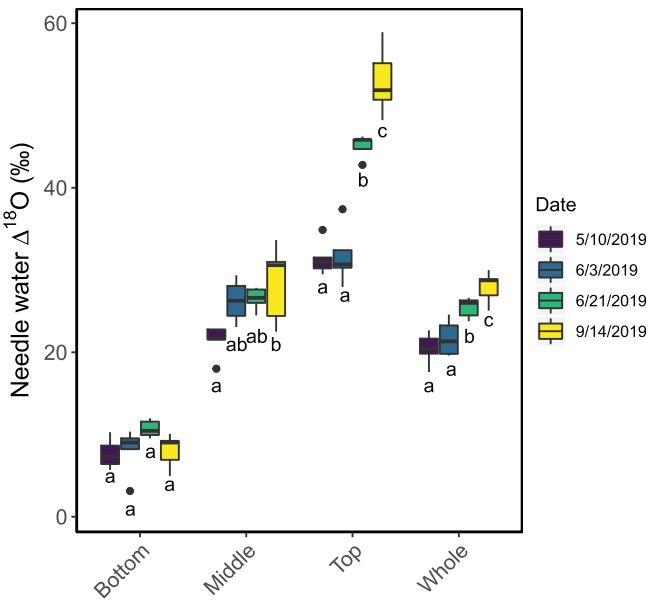

FIGURE 3 Seasonal variation in the progressive isotope enrichment effect for needles of *P. ponderosa*. $n = 5$ across different sampling dates within a given segment. Letter notation indicates significant pairwise differences between $\Delta^{18}O$ in the corresponding needle segment across different sampling dates (adjusted $\alpha = .05$). Horizontal lines within each box represent the median, boxes represent the limits of the lower and upper quartiles, vertical lines represent upper and lower ranges and dots represent outliers [Colour figure can be viewed at wileyonlinelibrary.com]

Despite seasonal variation in progressive enrichment that was associated with changes in RH, we observed little variation in progressive enrichment diurnally (Figure 4). In 2018, the magnitude of progressive isotope enrichment in both *P. contorta* and *P. ponderosa* did not differ throughout the day, nor was the magnitude of progressive enrichment different between the two species ($p > .05$ for all pairwise comparisons). Likewise, for *P. ponderosa* in 2019 the magnitude of progressive enrichment did not change diurnally. However, the overall magnitude of this base to tip enrichment across all time points was much lower for *P. ponderosa* in 2019 than in 2018, concomitant with ~50% higher RH during sampling periods as compared to 2018. Despite the large fluctuations in RH that occurred diurnally, the progressive enrichment effect was static on daily time scales, and thus we did not observe significant correlations between the degree of progressive enrichment and RH in 2018 ($p = .1$ for *P. contorta*, $p = .91$ for *P. ponderosa*) and only a weak relationship between RH and progressive enrichment in 2019 for *P. ponderosa* ($p = .05$, $R^2 = 0.27$).

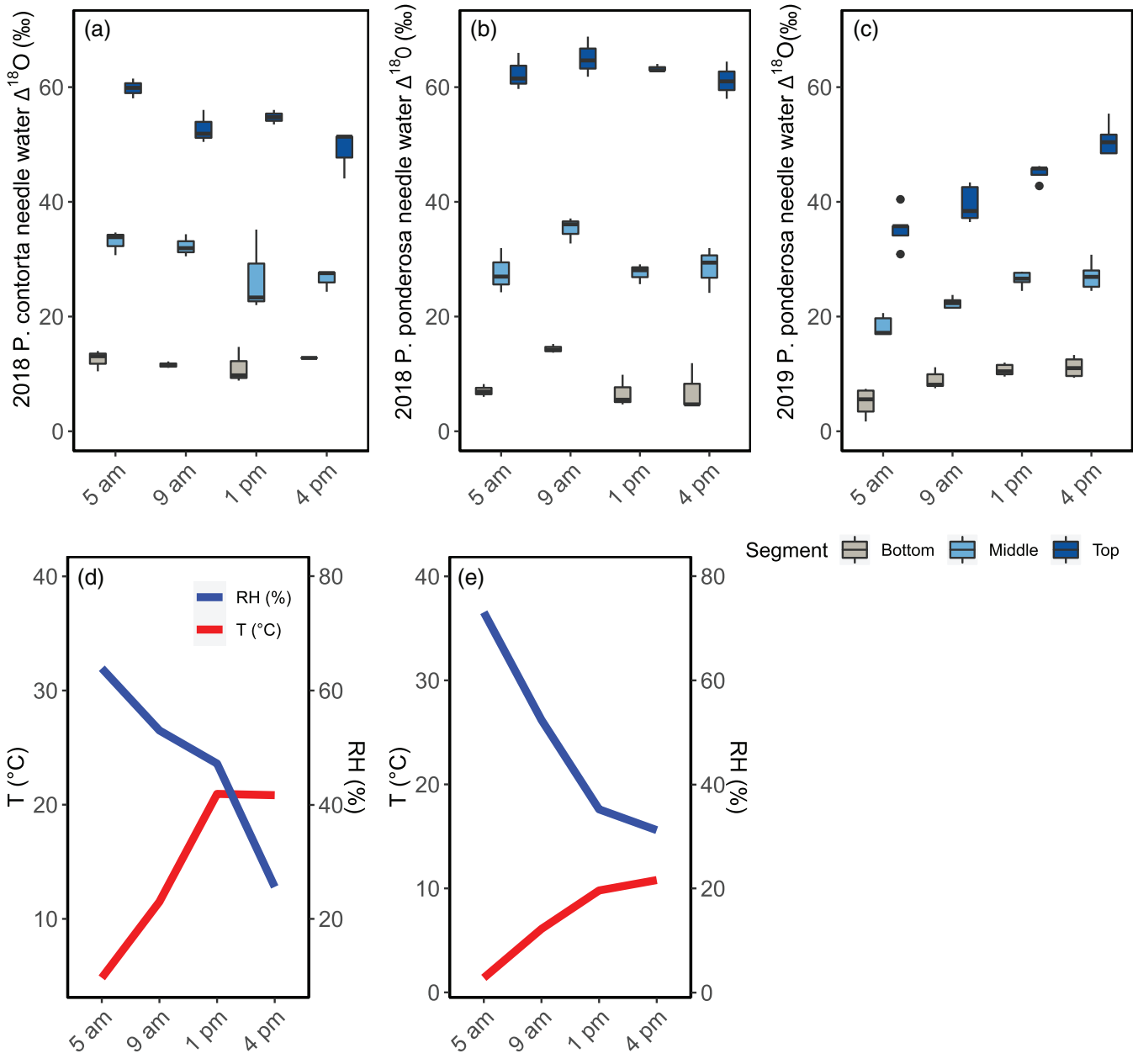

FIGURE 4 Diurnal variation in the progressive isotope enrichment effect for *P. contorta* in 2018 (a), *P. ponderosa* in 2018 (b) and *P. ponderosa* in 2019 (c). $n = 5$ for all sampling times and dates. Panels (d) and (e) represent temperature and relative humidity during sampling periods in 2018 and 2019, respectively. No significant pairwise differences exist between the magnitude of progressive enrichment across sampling times (adjusted $\alpha = .05$). Horizontal lines within each box represent the median, boxes represent the limits of the lower and upper quartiles, vertical lines represent upper and lower ranges and dots represent outliers [Colour figure can be viewed at wileyonlinelibrary.com]

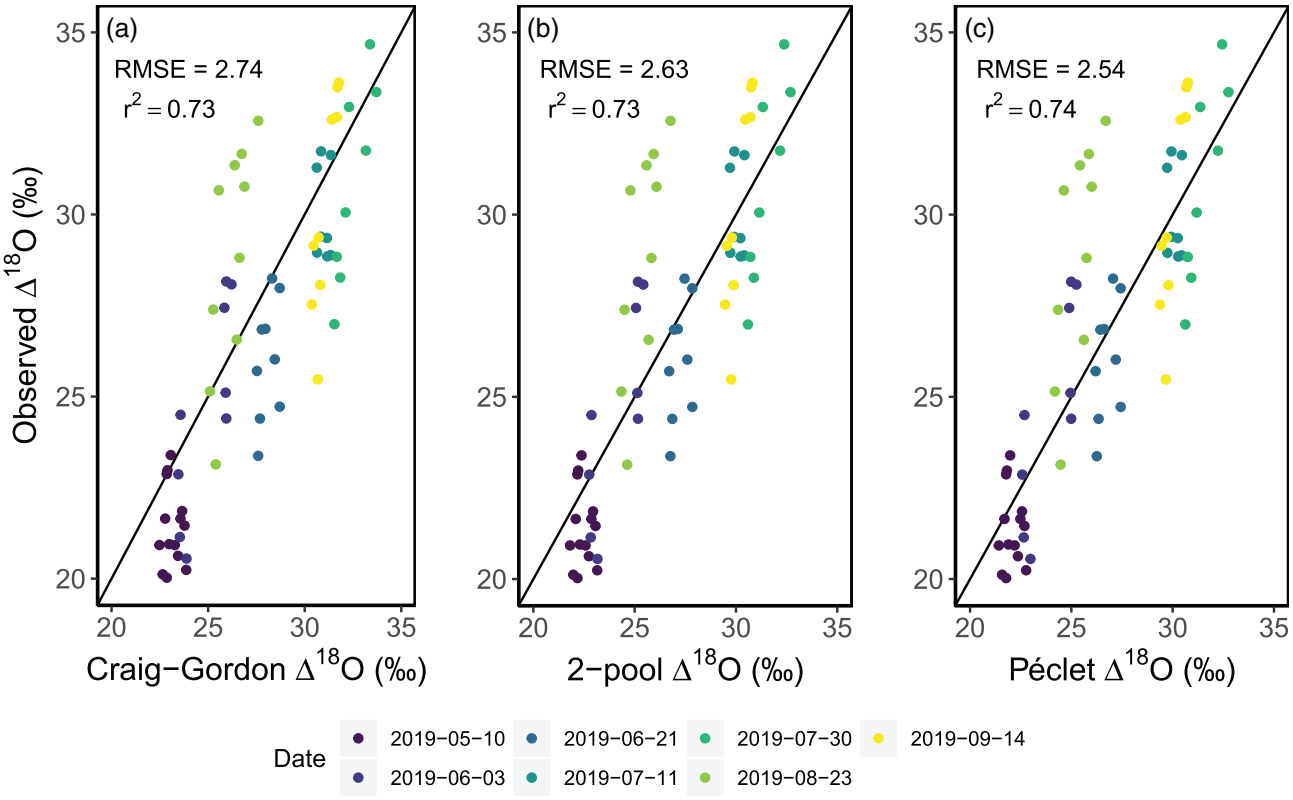

FIGURE 5 Observed bulk needle $\Delta^{18}O$ values and $\Delta^{18}O$ predictions for needles of *P. ponderosa* using the (a) unmodified C–G model, (b) the 2-pool C–G model and (c) the Péclet modification. Data are from the afternoon (1300 and 1600 hr) across all sampling dates. The black line represents a 1:1 trendline [Colour figure can be viewed at wileyonlinelibrary.com]

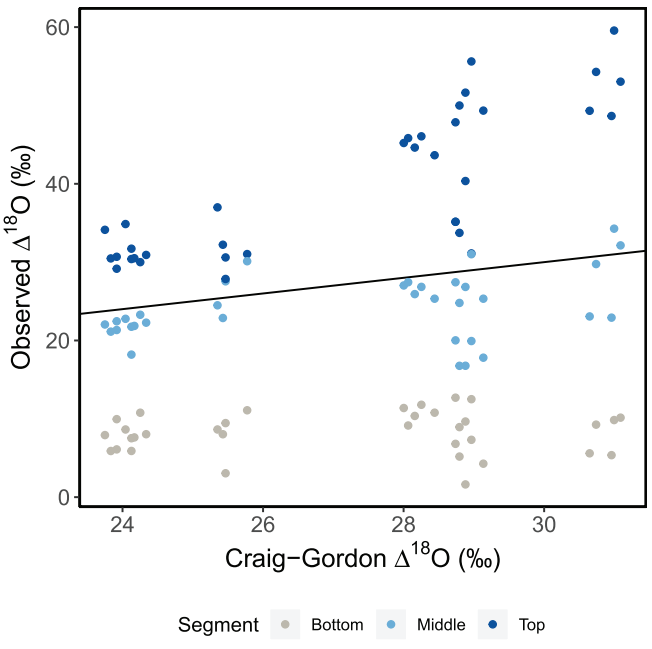

FIGURE 6 Observed $\Delta^{18}O$ values and $\Delta^{18}O$ predictions from the unmodified C–G model for all needle segments of *P. ponderosa*. Data are from the afternoon (1300 and 1600 hr) on all four sampling dates. The black line represents a 1:1 trendline [Colour figure can be viewed at wileyonlinelibrary.com]

3.3 | Model performance

In general, the unmodified C–G model worked well to predict bulk needle water enrichment seasonally (Figure 5a, RMSE = 2.74, R^2 = 0.73). However, the model tended to underpredict morning enrichment in August and September (Figure S3), likely a result of either (a) incomplete leaf water turnover overnight (i.e. non-steady-state effects), resulting in the retention of enriched water from the previous day (e.g. Lai, Ehleringer, Bond, & Paw, 2006), or (b) small lags in when samples were taken relative to our weather data averaging period, error that would be exacerbated around 0900 hr since that was when modelled $\Delta^{18}O$ most rapidly increased (Figure S3). Thus, we elected to use afternoon data for validating model predictions. When optimizing the parameters of the 2-pool C–G model (Figure 5b, f_u = 0.03, RMSE = 2.63, R^2 = 0.73) and the Péclet modification (Figure 5c, L = 0.006, RMSE = 2.54, R^2 = 0.74) to minimize model error, we found that these models slightly reduced RMSE but did not substantially increase R^2 as compared to the unmodified C–G predictions. For all three models, the discrepancy between observed and modelled bulk needle water enrichment was not associated with any particular meteorological conditions, nor was it associated with the magnitude of progressive enrichment. The success of the C–G model in predicting bulk needle enrichment, despite the presence of a large progressive enrichment effect, was likely due to its ability to

accurately model the average needle water (Figure 6), which tended to occur near the middle of the needle.

4 | DISCUSSION

Understanding the ubiquity, magnitude, and variation in the progressive enrichment of leaf water $\delta^{18}O$ are key steps towards resolving the mechanistic drivers of leaf water enrichment and informing best practices of leaf water isotope modelling. We found that progressive enrichment of needle water $\delta^{18}O$ (i.e. the difference between needle tip and base $\delta^{18}O$), was large in magnitude. In fact, the spatial variation in $\delta^{18}O$ along the length of *P. contorta* and *P. ponderosa* needles was always greater than variation associated with diurnal or seasonal fluctuations in environmental conditions. The large progressive enrichment of needle water $\delta^{18}O$ occurred across a wide range of conditions, including night, day, spring, summer, and fall, as well as across a wide range of temperature and humidity. Moreover, the effect was similar in magnitude in both species, despite *P. contorta* possessing needles only half the length of those in *P. ponderosa*. We also found a discontinuity in the drivers of progressive isotope enrichment, whereby decreases in RH resulted in greater progressive enrichment over the course of a season, yet similar fluctuations in RH diurnally only slightly (and inconsistently) altered progressive enrichment.

There has been much debate in the literature regarding the anatomical and environmental factors that cause variation in the magnitude of progressive isotope enrichment. For example, it has been suggested that increased leaf length (Helliker & Ehleringer, 2000; Ogée et al., 2007; Shu, Feng, Posmentier, Faiia, et al., 2008) and small interveinal distances in the leaf (largely present in C_4 grasses, Helliker & Ehleringer, 2000; Ogée et al., 2007) should increase the magnitude of progressive enrichment. However, our results run counter to these suggestions, as we observed that progressive isotope enrichment occurred at similar magnitudes in two species of conifer that differ in needle length by a factor of two. These observations suggest that longer needles do not necessarily lead to larger progressive enrichment effects. Instead, we found that the primary driver of greater progressive enrichment was seasonal decreases in RH, consistent with the 'desert river' type model that focuses on atmospheric humidity and needle transpiration rates as drivers of progressive enrichment (e.g. Farquhar & Gan, 2003; Ogée et al., 2007).

Current models of progressive enrichment provide insight regarding the anatomical features that cause this effect in conifers. For example, the Farquhar and Gan (2003) model suggests that the progressive isotope enrichment effect itself arises only when the ratio of water advection to diffusion (i.e. the Péclet number) is large longitudinally but small radially. This would appear to be the case particularly in some conifers, as a consequence of the endodermis and Casparian strip that surrounds needle xylem. This anatomical trait directs bulk water flow longitudinally while reducing water advection radially (Liesche, Martens, & Schulz, 2011; Roden et al., 2015), relying on aquaporins to mediate radial water transport (Laur & Hacke, 2014). This slow radial advection would allow the heavy isotopologue to more easily diffuse from stomatal evaporative sites, through aquaporins, and back into the xylem water, further enriching the longitudinal flow (Farquhar & Gan, 2003; Ogée et al., 2007). In conifers, this combination of 'desert river' type longitudinal flow, a Casparian strip, and aquaporins may be the key anatomical features that cause large progressive enrichment effects that are similar in magnitude across species, while seasonal fluctuations in RH cause additional variation in $\delta^{18}O$ along the length of the needle.

These results are most relevant for examining the factors that cause progressive enrichment in *Pinus* species, but large spatial variation in leaf water $\delta^{18}O$ has also been documented in C_3 and C_4 grasses (Gan et al., 2002, 2003; Helliker & Ehleringer, 2000, 2002), cacti (Cernusak et al., 2016), and angiosperm tree species (Gerlein-Safdi, Gauthier, Sinkler, & Caylor, 2017; Šantrůček et al., 2007). While the anatomical and physiological features promoting progressive enrichment in various species may differ, it is clear that this phenomenon is widespread across a wide taxonomic range of species. Future work is needed to explore the mechanisms that cause large progressive isotope enrichment effects across a diverse assemblage of taxa.

Our data provide insight into two key predictions from the Farquhar and Gan (2003) 'desert river' model. Firstly, we found that bulk needle water $\Delta^{18}O$ closely matched enrichment in the middle segment at all times of the year. The average $\Delta^{18}O$ value integrated along the leaf from the 'desert river' model is identical to the bulk C–G prediction; given a linear increase in isotope ratios along the needle and homogeneous leaf water content, the average isotope enrichment is likely to be found near the middle. This linear increase in $\Delta^{18}O$ along the length of a needle is common in the Farquhar and Gan (2003) model, though there are certain conditions (primarily high humidity and low temperature) that could dampen the magnitude of tip enrichment and cause the average enrichment to be shifted towards the base of the needle. We did observe a non-linearity in progressive enrichment in our two earliest sampling points due to lower needle tip enrichment, though this non-linearity did not shift bulk needle $\Delta^{18}O$ to more closely match basal needle segments. Thus, while non-linearity versus linearity in progressive enrichment could have important implications for the accuracy of C–G models, we were not able to resolve this question in the present study. Secondly, we observed seasonal variation in progressive isotope enrichment to be most closely linked to variation in $\Delta^{18}O$ at the tip of the needle, a result also consistent with the Farquhar and Gan (2003) model. This observation could be due to changing boundary layer conditions along the length of the needle, since needles in *P. contorta* and *P. ponderosa* are more closely bundled at the base than at the tip. Therefore, needle segments closer to the branch may experience lower wind speeds and higher humidity than more distal segments. Additionally, the possibility exists that aspects of needle anatomy (e.g. water content or hydraulic architecture, Holloway-Phillips et al., 2016) or physiology (e.g. transpiration rate or aquaporin expression, Shu, Feng, Posmentier, Sonder, et al., 2008) could differ along the length of the needle, though this remains underexplored in leaves in general, let alone in conifers specifically.

One of the most surprising observations in our dataset is that the magnitude of progressive isotope enrichment was exacerbated under conditions of low RH, though this relationship occurred only over seasonal timescales and not diurnal timescales. Other studies have suggested that progressive enrichment should vary in accordance with humidity (Gan et al., 2002; Helliker & Ehleringer, 2000; Šantrůček et al., 2007), yet our observation that progressive enrichment is insensitive to fluctuations in humidity on short time scales is not consistent with those predictions. Moreover, our results run counter to previous work that suggested progressive enrichment should be largest during periods of high transpiration (Šantrůček et al., 2007), which would not occur at night due to low stomatal conductance. There are a few explanations for this counterintuitive observation. Firstly, non-steady-state conditions and slow leaf water turnover times at night (Lai et al., 2006; Simonin et al., 2013; Wang & Yakir, 1995), potentially caused by hydraulic compartmentalization between conifer veins and mesophyll (Cernusak et al., 2016; Zwieniecki, Brodribb, & Holbrook, 2007), could cause any daytime leaf water enrichment patterns to persist throughout the night. While models have been developed to account for non-steady-state effects, this explanation would not be entirely consistent with our observations of large diurnal variability in bulk leaf water $\Delta^{18}O$, which would indicate that leaf water turnover was at least partially occurring. Secondly, progressive enrichment may not actually be sensitive to RH and instead seasonal increases in progressive enrichment could be due to a buildup of hydraulic damage that would increase tortuosity and the radial path length of leaf water (Ferrio et al., 2012). In support of this hypothesis, we observed that the magnitude of progressive enrichment was larger in late June than in early June, despite higher RH at the end of the month. Other age-related trends in needle anatomy could also cause progressive enrichment to increase seasonally, although we only sampled older needles that were unlikely to undergo rapid anatomical changes in the span of a few months. Finally, progressive enrichment may be static diurnally because, though stomata are largely closed at night, some water is still being lost from the needle at all times of the day, and this water loss is sufficient to drive progressive enrichment. Nocturnal transpiration is a well-documented process that occurs in many *Pinus* species (Caird, Richards, & Donovan, 2007; Yu, Goldsmith, Wang, & Anderegg, 2019) and could thus affect leaf water enrichment (Cuntz et al., 2007; Seibt, Wingate, & Berry, 2007). This slow but steady water loss from leaves would result in reduced radial water advection (relative to the higher radial advection during daytime transpiration) and thus an increased role of back-diffusion of heavy isotopologues, potentially causing progressive enrichment patterns. However, diffusion would also be lower at night due to lower temperature (though this effect is likely small), so it is difficult to draw any definitive conclusions about diurnal changes in the radial Péclet number. Ultimately, all of these factors could be at play during different times of the day and at different time scales. Understanding the interactions between water turnover time and the factors that cause large radial Péclet effects are a fruitful avenue for disentangling the specific mechanistic drivers of the progressive enrichment of leaf water.

Despite the size of the progressive isotope enrichment effect, we found that the C–G model was sufficient to explain variation in bulk needle water enrichment. While the common 2-pool or longitudinal Péclet modifications did decrease model-data error slightly, it was a minor decrease and was due to only two sampling days during the season where the original C–G model overpredicted $\Delta^{18}O$. Considering that the 2-pool and Péclet modifications were developed to correct for systematic overpredictions in $\Delta^{18}O$ that should occur across all sampling dates, we believe there is no a priori reason to conclude that either of these models performed better than the unmodified C–G model. Since the unmodified C–G model did not systematically overpredict $\Delta^{18}O$, we observed smaller estimates of the unenriched water pool (f_u) and path length (L) than previous studies (Roden et al., 2015). While the two-pool and Péclet corrections have improved the accuracy of C–G prediction in some past studies (e.g. Cernusak et al., 2016; Roden et al., 2015), our results add to recent evidence that challenges the use of these corrections for predicting bulk leaf water enrichment in conifers. For example, Belmecheri et al. (2018) found that an unmodified Craig–Gordon model outperformed the two-pool and Péclet models in *P. ponderosa* needles. In contrast, Roden et al. (2015) found that both corrections were necessary to get the best fit between modelled and measured $\Delta^{18}O$ in six conifer species, but that the path length necessary in the Péclet correction varied throughout time and was substantially longer than could be accounted for by anatomical distances alone. Finally, it is worth noting that while the C–G models predicted bulk needle water $\Delta^{18}O$ quite well across the season, there is still a large amount of unexplained variation in observed $\Delta^{18}O$ within any given day, likely due to microclimate differences between the meteorological station and the branches we sampled. Our results, in conjunction with previous research, indicates that leaf water isotope modelling in conifers continues to be subject to numerous uncertainties, and that the common 2-pool and Péclet modifications are not always necessary to successfully predict bulk needle water $\Delta^{18}O$.

In sum, we found progressive isotope enrichment of needle water to be present and large both seasonally and diurnally in two conifer species. This enrichment pattern is hypothesized to be due to unique elements of conifer needle anatomy and water loss, which contribute to a consistent radial, backward diffusion of enriched water from the stomata to the xylem, combined with a 'desert river' type of longitudinal flow. However, the precise anatomical and physiological factors that anchor this hypothesis remain to be characterized, as well as its prevalence in other plant taxa. Despite the large progressive enrichment effect, we found that the foundational C–G model successfully predicted variation in bulk needle water enrichment, especially across seasonal time scales. Thus, it appears that the C–G model is able to capture the thermodynamic processes that drive bulk leaf water enrichment despite omitting fundamental mechanisms that could cause large variability in $\delta^{18}O$ within a given leaf.

The development of more complex leaf water enrichment models has largely been motivated by: (a) a desire to increase our ability to predict leaf water enrichment across a wide variety of species and meteorological conditions (Cernusak et al., 2016), and (b) developing insight regarding water transport pathways (Barbour, Farquhar, & Buckley, 2017). Here, we show that the C–G model is generally sufficient to predict bulk $\Delta^{18}O$ in conifer needles. However, the static nature of progressive enrichment

diurnally despite the dynamic nature of progressive enrichment seasonally suggests previously unrecognized sources of variation in progressive isotope enrichment that could be due to the unique ways that water moves through leaves at night. Studies that investigate how rapidly manipulating the meteorological conditions around the needle (by bagging or other methods) alters nighttime versus daytime progressive enrichment would be valuable endeavours towards resolving these unknowns, as would studies that sample continuously over a few weeks to uncover the precise time scale over which humidity alters the magnitude of progressive enrichment. We further suggest that the temporal variability in progressive enrichment, and the implications of this effect for leaf hydraulics, be investigated both via new methodologies to visualize water movement in leaves (e.g. Defraeye et al., 2014), and by expanded datasets across a wide variety of conditions and species.

Leaf water $\Delta^{18}O$ imparts its isotopic signature on many downstream processes including phloem sugars (Bögelein, Lehmann, & Thomas, 2019), needle cellulose (Wright & Leavitt, 2006) and tree-ring cellulose (Roden et al., 2000). Given the magnitude of progressive isotope enrichment and the ample evidence for its prevalence, it is surprising that (to our knowledge) only one study has sought to track the implications of progressive enrichment of leaf water for leaf cellulose isotope ratios (Helliker & Ehleringer, 2002). Additionally, it is yet unknown how the progressive enrichment of leaf water may affect the isotopic ratios of exported sugars. If exported sugars reflect the isotopic signal from certain parts of the leaf more strongly (as suggested by Lehmann et al., 2017), the progressive enrichment effect could provide an explanation for the frequent decoupling between leaf water $\delta^{18}O$ and phloem organic matter (Barnard et al., 2007; Gessler et al., 2013). If this effect does indeed propagate to impact the isotopic ratios of downstream metabolic products, then current models of tree-ring isotope ratios may need to be reconsidered.

ACKNOWLEDGMENTS

We would like to thank Suvankar Chakraborty for his extensive assistance with isotopic measurements. We also thank Emily Johnson, Avery Driscoll and Nicolas Bitter for helping with field data collection and water extractions. Funding for this work was provided by the NSF DEB Ecosystem Science cluster, grants 1753845 and 1754430. William R. L. Anderegg also acknowledges funding from the David and Lucille Packard Foundation, NSF grant 1714972, and the USDA National Institute of Food and Agriculture, Agricultural and Food Research Initiative Competitive Program, Ecosystem Services and Agro-ecosystem Management, grant 2018-67019-27850. Richard P. Fiorella and William R. L. Anderegg also acknowledge funding from NSF grant 1802880.

CONFLICT OF INTEREST

The authors declare no conflicts of interest.

ORCID

Steven A. Kannenberg https://orcid.org/0000-0002-4097-9140
Richard P. Fiorella https://orcid.org/0000-0002-0824-4777
William R. L. Anderegg https://orcid.org/0000-0001-6551-3331
James R. Ehleringer https://orcid.org/0000-0003-2050-3636

REFERENCES

Barbour, M. M., Farquhar, G. D., & Buckley, T. N. (2017). Leaf water stable isotopes and water transport outside the xylem. *Plant Cell and Environment*, *40*, 914–920.

Barnard, R. L., Salmon, Y., Kodama, N., Sörgel, K., Holst, J., Rennenberg, H., … Buchmann, N. (2007). Evaporative enrichment and time lags between δ18O of leaf water and organic pools in a pine stand. *Plant, Cell and Environment*, *30*, 539–550.

Belmecheri, S., Wright, W. E., Szejner, P., Morino, K. A., & Monson, R. K. (2018). Carbon and oxygen isotope fractionations in tree rings reveal interactions between cambial phenology and seasonal climate. *Plant, Cell & Environment*, *41*, 2758–2772.

Bögelein R., Lehmann M.M. & Thomas F.M. (2019) Differences in carbon isotope leaf-to-phloem fractionation and mixing patterns along a vertical gradient in mature European beech and Douglas fir.

Caird, M. A., Richards, J. H., & Donovan, L. A. (2007). Nighttime stomatal conductance and transpiration in C3 and C4 plants. *Plant Physiology*, *143*, 4–10.

Cernusak, L. A., Barbour, M. M., Arndt, S. K., Cheesman, A. W., English, N. B., Feild, T. S., … Farquhar, G. D. (2016). Stable isotopes in leaf water of terrestrial plants. *Plant Cell and Environment*, *39*, 1087–1102.

Craig, H., & Gordon, L. (1965). Deuterium and oxygen-18 variations in the ocean and the marine atmosphere. In E. Tongiorgi (Ed.), *Proceedings of a conference on stable isotopes in oceanographic studies and palaeotemperature* (pp. 9–130). Pisa, Italy: Lischi and Figli.

Cuntz, M., Ogée, J., Farquhar, G. D., Peylin, P., & Cernusak, L. A. (2007). Modelling advection and diffusion of water isotopologues in leaves. *Plant, Cell and Environment*, *30*, 892–909.

Dawson, T. E., Mambelli, S., Plamboeck, A. H., Templer, P. H., & Tu, K. P. (2002). Stable isotopes in plant ecology. *Annual Review of Ecology and Systematics*, *33*, 507–559.

Defraeye, T., Derome, D., Aregawi, W., Cantré, D., Hartmann, S., Lehmann, E., … Nicolai, B. (2014). Quantitative neutron imaging of water distribution, venation network and sap flow in leaves. *Planta*, *240*, 423–436.

Dole, M., Lane, G., Rudd, D., & Zaukelies, D. (1954). Isotopic composition of atmospheric oxygen and nitrogen. *Geochimica et Cosmochimica Acta*, *6*, 65–78.

Dongmann, G., Nurnberg, H., Forstel, H., & Wagener, K. (1974). On the enrichment of H128O in the leaves of transpiring plants. *Radiation and Environmental Biophysics*, *11*, 41–52.

Ehleringer, J. R., Roden, J. S., & Dawson, T. E. (2000). Assessing ecosystem-level water relations through stable isotope ratio analysis. In O. E. Sala, R. B. Jackson, H. A. Mooney, & R. Howarth (Eds.), *Methods in ecosystem science* (2nd ed.). New York, NY: Springer.

Farquhar, G., & Gan, K. (2003). On the progressive enrichment of the oxygen isotopic composition of water along a leaf. *Plant, Cell & Environment*, *26*, 1579–1597.

Farquhar, G., & Lloyd, J. (1993). Carbon and oxygen isotope effects in the exchange of carbon dioxide between terrestrial plants and the atmosphere. In J. Ehleringer, A. Hall, & G. Farquhar (Eds.), *Stable isotopes and plant carbon–water relations* (pp. 47–70). San Diego, CA: Academic Press.

Farquhar, G. D., & Cernusak, L. A. (2005). On the isotopic composition of leaf water in the non-steady state. *Functional Plant Biology*, *32*, 293–303.

Ferrio, J. P., Pou, A., Florez-Sarasa, I., Gessler, A., Kodama, N., Flexas, J., & Ribas-Carbó, M. (2012). The Péclet effect on leaf water enrichment correlates with leaf hydraulic conductance and mesophyll conductance for CO_2. *Plant, Cell and Environment*, *35*, 611–625.

Fiorella, R., Bares, R., Lin, J., Ehleringer, J., & Bowen, G. (2018). Detection and variability of combustion-derived vapor in an urban basin. *Atmospheric Chemistry and Physics*, *18*, 8529–8547.

Fiorella, R., West, J., & Bowen, G. (2019). Biased estimates of the isotope ratios of steady-state evaporation from the assumption of equilibrium between vapour and precipitation. *Hydrological Processes*, *33*, 2576–2590.

Flanagan, L. B., Comstock, J. P., & Ehieringer, J. R. (1991). Comparison of modeled and observed environmental influences on the stable oxygen and hydrogen isotope composition of leaf water in *Phaseolus vulgaris* L. *Plant Physiology*, *96*, 588–596.

Gan, K. S., Wong, S. C., Ong, J. W. H. Y., & Farquhar, G. D. (2003). Evaluation of models of leaf water 18O enrichment using measurements of spatial patterns of vein xylem water, leaf water and dry matter in maize leaves. *Plant, Cell and Environment*, *26*, 1479–1495.

Gan, K. S., Wong, S. C., Yong, J. W. H., & Farquhar, G. D. (2002). 18O spatial patterns of vein xylem water, leaf water, and dry matter in cotton leaves. *Plant Physiology*, *130*, 1008–1021.

Gehre, M., Geilmann, H., Richter, J., Werner, R. A., & Brand, W. A. (2004). Continuous flow 2H/1H and 18O/16O analysis of water samples with dual inlet precision. *Rapid Communications in Mass Spectrometry*, *18*, 2650–2660.

Gerlein-Safdi, C., Gauthier, P. P. G., Sinkler, C. J., & Caylor, K. K. (2017). Leaf water 18O and 2H maps show directional enrichment discrepancy in *Colocasia esculenta*. *Plant Cell and Environment*, *40*, 2095–2108.

Gessler, A., Brandes, E., Keitel, C., Boda, S., Kayler, Z. E., Granier, A., … Treydte, K. (2013). The oxygen isotope enrichment of leaf-exported assimilates - Does it always reflect lamina leaf water enrichment? *New Phytologist*, *200*, 144–157.

Helliker, B. R., & Ehleringer, J. R. (2000). Establishing a grassland signature in veins: 18O in the leaf water of C3 and C4 grasses. *Proceedings of the National Academy of Sciences of the United States of America*, *97*, 7894–7898.

Helliker, B. R., & Ehleringer, J. R. (2002). Differential 18O enrichment of leaf cellulose in C3 versus C4 grasses. *Functional Plant Biology*, *29*, 435–442.

Holloway-Phillips, M., Cernusak, L. A., Barbour, M., Song, X., Cheesman, A., Munksgaard, N., … Farquhar, G. D. (2016). Leaf vein fraction influences the Péclet effect and 18O enrichment in leaf water. *Plant Cell and Environment*, *39*, 2414–2427.

Horel, J., Splitt, M., Dunn, L., Pechmann, J., White, B., Ciliberti, C., … Burks, J. (2002). Mesowest: Cooperative mesonets in the western United States. *Bulletin of the American Meteorological Society*, *83*, 211–226.

Horita, J., & Wesolowski, D. (1994). Liquid–vapor fractionation of oxygen and hydrogen isotopes of water from the freezing to the critical temperature. *Geochimica et Cosmochimica Acta*, *58*, 3425–3437.

Kahmen, A., Schefuß, E., & Sachse, D. (2013). Leaf water deuterium enrichment shapes leaf wax *n*-alkane δd values of angiosperm plants I: Experimental evidence and mechanistic insights. *Geochimica et Cosmochimica Acta*, *111*, 39–49.

Kolb, T. E., Holmberg, K. M., Wagner, M. R., & Stone, J. E. (1998). Regulation of ponderosa pine foliar physiology and insect resistance mechanisms by basal area treatments. *Tree Physiology*, *18*, 375–381.

Lai, C. T., Ehleringer, J. R., Bond, B. J., & Paw, U. K. T. (2006). Contributions of evaporation, isotopic non-steady state transpiration and atmospheric mixing on the δ18O of water vapour in Pacific northwest coniferous forests. *Plant, Cell and Environment*, *29*, 77–94.

Laur, J., & Hacke, U. G. (2014). Exploring *Picea glauca* aquaporins in the context of needle water uptake and xylem refilling. *New Phytologist*, *203*, 388–400.

Leaney, F., Osmond, C., Allison, G., & Ziegler, H. (1985). Hydrogen-isotope composition of leaf water in C3 and C4 plants: Its relationship to the hydrogen-isotope composition of dry matter. *Planta*, *164*, 215–220.

Lehmann, M. M., Gamarra, B., Kahmen, A., Siegwolf, R. T. W., & Saurer, M. (2017). Oxygen isotope fractionations across individual leaf carbohydrates in grass and tree species. *Plant Cell and Environment*, *40*, 1658–1670.

Liesche, J., Martens, H. J., & Schulz, A. (2011). Symplasmic transport and phloem loading in gymnosperm leaves. *Protoplasma*, *248*, 181–190.

Merlivat, L. (1978). Molecular diffusivities of H216O, HD16O and H218O in Gases. *The Journal of Chemical Physics*, *69*, 2864–2871.

Nelson, S. T. (2000). A simple, practical methodology for routine VSMOW/SLAP normalization of water samples analyzed by continuous flow methods. *Rapid Comminications in Mass Spectrometry*, *14*, 1044–1046.

Ogée, J., Cuntz, M., Peylin, P., & Bariac, T. (2007). Non-steady-state, non-uniform transpiration rate and leaf anatomy effects on the progressive stable isotope enrichment of leaf water along monocot leaves. *Plant, Cell and Environment*, *30*, 367–387.

R Core Team (2019). *R: A language and environment for statistical computing*, Vienna, Austria: R Foundation for Statistical Computing. https://www.R-project.org/

Roden, J., & Ehleringer, J. (1999). Observations of hydrogen and oxygen isotopes in leaf water confirm the Craig–Gordon model under wide-ranging environmental conditions. *Plant Physiology*, *120*, 1165–1173.

Roden, J., Kahmen, A., Buchmann, N., & Siegwolf, R. (2015). The enigma of effective path length for 18O enrichment in leaf water of conifers. *Plant Cell and Environment*, *38*, 2551–2565.

Roden, J. S., Lin, G., & Ehleringer, J. R. (2000). A mechanistic model for interpretation of hydrogen and oxygen isotope ratios in tree-ring cellulose. *Geochimica et Cosmochimica Acta*, *64*, 21–35.

Šantrůček, J., Květoň, J., Šetlík, J., & Bulíčková, L. (2007). Spatial variation of deuterium enrichment in bulk water of snowgum leaves. *Plant Physiology*, *143*, 88–97.

Seibt, U., Wingate, L., & Berry, J. A. (2007). Nocturnal stomatal conductance effects on the δ18O signatures of foliage gas exchange observed in two forest ecosystems. *Tree Physiology*, *27*, 585–595.

Shu, Y., Feng, X., Posmentier, E. S., Faiia, A. M., Ayres, M. P., Conkey, L. E., & Sonder, L. J. (2008). Isotopic studies of leaf water. Part 2: Between-age isotopic variations in pine needles. *Geochimica et Cosmochimica Acta*, *72*, 5189–5200.

Shu, Y., Feng, X., Posmentier, E. S., Sonder, L. J., Faiia, A. M., & Yakir, D. (2008). Isotopic studies of leaf water. Part 1: A physically based two-dimensional model for pine needles. *Geochimica et Cosmochimica Acta*, *72*, 5175–5188.

Simonin, K. A., Roddy, A. B., Link, P., Apodaca, R., Tu, K. P., Hu, J., … Barbour, M. M. (2013). Isotopic composition of transpiration and rates of change in leaf water isotopologue storage in response to environmental variables. *Plant, Cell and Environment*, *36*, 2190–2206.

Song, X., Loucos, K. E., Simonin, K. A., Farquhar, G. D., & Barbour, M. M. (2015). Measurements of transpiration isotopologues and leaf water to assess enrichment models in cotton. *New Phytologist*, *206*, 637–646.

Wang, X., & Yakir, D. (1995). Temporal and spatial variation in the oxygen-18 content of leaf water in different plant species. *Plant, Cell and Environment*, *18*, 1377–1385.

Welp, L. R., Keeling, R. F., Meijer, H. A. J., Bollenbacher, A. F., Piper, S. C., Yoshimura, K., … Wahlen, M. (2011). Interannual variability in the oxygen isotopes of atmospheric CO_2 driven by El Niño. *Nature*, *477*, 579–582.

West, A. G., Patrickson, S. J., & Ehleringer, J. R. (2006). Water extraction times for plant and soil materials used in stable isotope analysis. *Rapid Communications in Mass Spectrometry*, *20*, 1317–1321.

Wright, W. E., & Leavitt, S. W. (2006). Needle cell elongation and maturation timing derived from pine needle cellulose δ18O. *Plant, Cell and Environment*, *29*, 1–14.

Yakir, D., DeNiro, M., & Gat, J. (1990). Natural deuterium and oxygen-18 enrichment in leaf water of cotton plants grown under wet and dry conditions: Evidence for water compartmentation and its dynamic. *Plant, Cell and Environment*, *13*, 49–56.

Yu, K., Goldsmith, G. R., Wang, Y., & Anderegg, W. R. L. (2019). Phylogenetic and biogeographic controls of plant nighttime stomatal conductance. *New Phytologist*, *222*, 1778–1788.

Zwieniecki, M. A., Brodribb, T. J., & Holbrook, N. M. (2007). Hydraulic design of leaves: Insights from rehydration kinetics. *Plant, Cell and Environment*, *30*, 910–921.

SUPPORTING INFORMATION

Additional supporting information may be found online in the Supporting Information section at the end of this article.

How to cite this article: Kannenberg SA, Fiorella RP, Anderegg WRL, Monson RK, Ehleringer JR. Seasonal and diurnal trends in progressive isotope enrichment along needles in two pine species. *Plant Cell Environ*. 2020;1–13. https://doi.org/10.1111/pce.13915